ORIGINAL ARTICLE

Nr 2025;15 (2):162-173

The Influence of Fetal Programming due to Maternal Obesity and Periodontitis on the Extensor Digitorum Longus Muscle of Wistar Rats

Gabriella Lopes Cappellaro[1], Thayná Náthally Petry de Paula[2], Mikael Gerson Kuhn[1], Rafaella Cristina Lima da Silva[3], Carlos Augusto Nassar[2], Rose Meire Costa[4], Lucinéia de Fátima Chasko Ribeiro[4], Sandra Lucinei Balbo[5], Ana Tereza Bittencourt Guimarães[6], Marcia Miranda Torrejais[1]

[1] *Experimental Laboratory of Morphology, Center for Medical and Pharmaceutical Sciences, Universidade Estadual do Oeste do Paraná, Cascavel, Paraná, Brazil*
[2] *Dentistry Course, Center for Biological and Health Sciences, Universidade Estadual do Oeste do Paraná, Cascavel, Paraná, Brazil*
[3] *Degree in Biological Sciences, Center for Biological and Health Sciences, Universidade Estadual do Oeste do Paraná, Cascavel, Paraná, Brazil*
[4] *Laboratory of Structural and Functional Biology, Center for Biological and Health Sciences, Universidade Estadual do Oeste do Paraná, Cascavel, Paraná, Brazil*
[5] *Laboratory of Endocrine Physiology and Metabolism, Center for Biological and Health Sciences, Universidade Estadual do Oeste do Paraná, Cascavel, Paraná, Brazil*
[6] *Biological Research Laboratory, Center for Biological and Health Sciences, Universidade Estadual do Oeste do Paraná, Cascavel, Paraná, Brazil*

CORRESPONDING AUTHOR:
Gabriella Lopes Cappellaro
Experimental Laboratory of Morphology
Center for Medical and Pharmaceutical Sciences
Universidade Estadual do Oeste do Paraná
Rua Universitária 2069
Jardim Universitário
85819-110 Cascavel (PR), Brazil
E-mail: gabycappellaro@hotmail.com

DOI:
10.32098/mltj.02.2025.06

LEVEL OF EVIDENCE: N/A (Animal study)

SUMMARY

Introduction. The aim of this study was to analyze the effects of fetal programming due to maternal obesity and/or periodontitis (PD) on the morphology and morphometry of the extensor digitorum longus (EDL) muscle in adult offspring of Wistar rats.

Methods. Twenty pregnant Wistar rats were used for formation of the parental generation: one group was injected with monosodium glutamate to induce obesity (MSG, n = 30), while the control group received hyperosmotic saline (CTL, n = 30). After 70 days, 15 animals of each group were induced of PD by ligature. The animals were reassigned to four groups and crossed to form the F1 generation (n = 7/group). The offspring of dams with PD were subjected to PD induction by ligature at 90 days of age. At 120 days, the animals were euthanized, and the EDL muscle was collected and weighed for study.

Results. The MSG/PD-F1 group showed a reduction in body weight compared to the PD-F1 group, as well as in retroperitoneal and periepididymal fat and EDL length compared to the MSG-F1 and PD-F1 groups. The muscle fibers had central nuclei and an amorphous shape, with differential staining in the groups with the diseases. There were significant differences in fiber density and capillary/fiber ratio between the PD-F1 and CTL-F1 groups. An increase in connective tissue was observed in the MSG-F1 group compared to CTL-F1 and in the MSG/ PD-F1 group compared to PD-F1.

Conclusions. The fetal programming due to maternal obesity and PD may affect body development and muscle function of the offspring.

KEY WORDS

Fetal development; monosodium glutamate; obesity; periodontal disease; skeletal muscle.

INTRODUCTION

Fetal programming refers to permanent or long-term changes in an organism as a result of stimuli or insults that occur during a certain critical period of life (1) such as the pre- and postnatal periods (childhood to adolescence), which are characterized by a high degree of plasticity (2). Fetal programming can be caused by different insults, including maternal and fetal diseases, nutritional alterations, medical interventions, smoking, and hypertension (3). These disturbances modify the development of the fetus through the so-called epigenetic mechanisms, which are molecular alterations that occur in DNA or in related proteins (2). These alterations have consequences for the following generations, immediately during postnatal life or remaining silent through to adult life (4).

Studies on fetal programming have provided important data regarding the origin of diseases that manifest in adults. Maternal nutrition is one of the factors that has attracted widespread attention, considering the increase in the global incidence of obesity (5). According to the World Health Organization (6), approximately 2.3 billion people worldwide are overweight or obese. In Brazil, about 96 million people are overweight (7).

During pregnancy, maternal exposure to high-fat diets can lead to systemic inflammation, affecting fetal development. Inflammatory cytokines such as TNF-α and IL-6 are often elevated in mothers who are overweight or obese, and this inflammation can influence the metabolic programming of the fetus (3, 8).

Obesity is a key factor in the development of metabolic syndrome (9). Furthermore, obesity is related to low-grade chronic systemic inflammation in adipose tissue, which is caused by activation of the immune system and triggers a proinflammatory state and local and systemic oxidative stress. This inflammatory condition is associated with the development of chronic diseases such as diabetes mellitus, cardiovascular and liver diseases, and periodontal diseases (10).

It is therefore important to study how the inflammatory condition in obesity is related to other diseases. One of such diseases is periodontal disease, which affects a large proportion of the population. Periodontal disease ranks 11th position in global prevalence, ranging from 20% to 50%, and is considered one of the most important oral diseases (11). It is an inflammatory and infectious disease that affects the supporting structures of the teeth. The most severe form is periodontitis (PD) (12).

Studies have shown that obesity contributes to the severity of PD (13, 14). The relationship between obesity and PD can be explained by the increase in the plasma concentration of proinflammatory cytokines. The release of cytokines by adipose tissue and by proinflammatory hormones can induce inflammatory processes and oxidative stress, which result in a similar pathophysiology of the two diseases (15). Excessive production of these cytokines can compromise the biomechanics of muscles and tendons, contributing to the development of tendinopathies and reducing functional capacity in individuals (16). However, the biological mechanism underlying this relationship is not fully understood and there is a lack of studies aimed at elucidating the effects of these systemic inflammatory diseases on muscle tissue integrity.

Skeletal muscle possesses adaptive capacity and plasticity that permit it to respond to stimuli or insults such as hormonal changes and maternal diseases that can affect muscle health (17). Compound muscles with a predominance of type II fibers show a predisposition to nutritional disorders. The extensor digitorum longus (EDL) muscle (18) is such a muscle and was used in the present study.

Therefore, this study aimed to analyze the effects of fetal programming due to maternal obesity and/or PD on the morphology and morphometry of the EDL muscle in adult offspring of female Wistar rats.

MATERIALS AND METHODS

This experimental, quantitative, randomized study was conducted at the Laboratory for the Study of Injuries and Physiotherapeutic Resources (LELRF) and at the Experimental Laboratory of Morphology (LABEM), State University of Western Paraná (UNIOESTE), Cascavel Campus. The local Ethics Committee approved all procedures involving animals on February 08, 2017.

Animals

For this study, pregnant Wistar rats (n = 20) were maintained under controlled conditions of temperature (23 ± 2 °C) and light (12-hour light/dark cycle, 7:00-19:00 h). The animals received water and standard chow throughout the experiment and were weighed once a week after weaning.

Characterization of groups and experimental design of dams

After the birth of the pups of the parental generation, only female rats were used for disease induction (obesity and PD), while male rats were separated for subsequent crossing. The female rats were divided into two groups: during the first 5 days of life, one group received subcutaneous injections of monosodium glutamate to induce obesity (MSG group, n = 30) and the control group received hypertonic saline solution (CTL group, n = 30) (19). At 70 days of age, the female rats were divided into four groups of 15 animals each; in two

groups, the animals were submitted to the induction of PD by ligature (20), corresponding to the parental generation (n = 60): control (CTL, n = 15), periodontitis (PD, n = 15), MSG-induced obesity (MSG, n = 15), and MSG-induced obesity + periodontitis (MSG/PD, n = 15). At 77 days of age, *i.e.*, 7 days after PD induction, five females per group were euthanized for the confirmation of PD by radiographic analysis and of obesity based on the Lee index and periepididymal and retroperitoneal fat weights. After confirmation, the females of all groups were crossed with the control rats at a ratio of one male to two females.

Pregnancy was confirmed by weighing and monitoring of the estrous cycle. After confirmation, the male rats were euthanized. The gestation and lactation period lasted 45 days and the dams were euthanized thereafter. Only male offspring composed the F1 generation and were divided into the following groups: control (CTL-F1), periodontitis (PD-F1), MSG-induced obesity (MSG-F1), and MSG-induced obesity + periodontitis (MSG/PD-F1). The PD-F1 and MSG/PD-F1 groups were submitted to the induction of PD by ligature at 90 days of age and were euthanized at 120 days (20). Obesity was not induced in the offspring groups.

Protocol for the induction and confirmation of obesity

During the first 5 days of life, animals of the parental generation were submitted to the protocol of obesity induction, which consisted of daily subcutaneous injections of 4 g MSG/kg in the neck region (MSG group, n = 30). Control animals received hypertonic saline solution (1.25 g/kg/day; CTL group, n = 30) (19).

Before euthanasia, obesity was confirmed by the measurement of body weight and nasoanal length for calculation of the Lee index {[body weight (g)/nasoanal length (cm)] × 1,000} (21, 22). After euthanasia, the retroperitoneal and periepididymal fat was collected and weighed on a digital scale. Relative fat accumulation was estimated by dividing these values by 100 g of body weight (g/100 g) (21). The fat weights were summed for statistical analysis.

Protocol for the induction and confirmation of periodontitis

For PD induction, the animals were anesthetized by intraperitoneal injection of 0.08 mg/kg ketamine hydrochloride (Dopalen®, Sespo Indústria e Comércio, Paulínia, SP) and 0.04 mg/kg xylazine hydrochloride (Anasedan®, Sespo Indústria e Comércio, Paulínia, SP). The animals were then positioned on an operating table, with the mouth being kept open to facilitate access to the teeth in the posterior mandible. Using modified tweezers and an exploratory probe, cotton thread number 40 (GLACE®) was placed around the right and left mandibular first molars. Ligature favors the accumulation of bacterial plaque, which is a gingival irritant (20). After the PD protocol, the animals were divided into four groups: control (CTL group), MSG-induced obesity (MSG group), periodontitis (PD group), and MSG-induced obesity + periodontitis (MSG/PD group). The disease was confirmed 7 days after induction and five females each in the PD and MSG/PD groups were euthanized. Offspring of the PD-F1 and MSG/PD-F1 groups were submitted to the PD protocol at 90 days of age; 30 days later, these animals were euthanized, and disease was confirmed by radiographic analysis.

After euthanasia, the left hemimandibles of each animal (dams and offspring) were removed and fixed in 10% formaldehyde for 48 hours. Next, the samples were washed under running water for 24 hours and kept in 70% alcohol. The hemimandibles were placed with the lingual side on a Kodak RVG 6100 digital radiographic sensor [image resolution of 20 lp/mm, theoretical resolution of sensor of 27.03 lp/mm, optical fiber 1, active surface dimensions of 22 × 30 mm, and matrix dimensions (pixels) of 1,200 × 1,600 (1.92 million)] and then positioned in such a way that the buccal and lingual cusps of the first molars were in the same vertical plane. A GE 1000 X-ray machine (15 mA, 65 Vp, 18 impulses, focus/film distance of 50 cm) was used, with the X-ray beam perpendicular to the specimens. From the digitized images, three linear measurements (in pixels) of the distance from the cementoenamel junction to the alveolar bone crest were obtained on the mesial side of the left mandibular first molar using the Image Pro Plus® program (Media Cybernetics, Maryland, USA) and the mean of these measurements was calculated (**figure 1**) (20). All measurements were made by a single examiner blinded to the identity of the experimental groups.

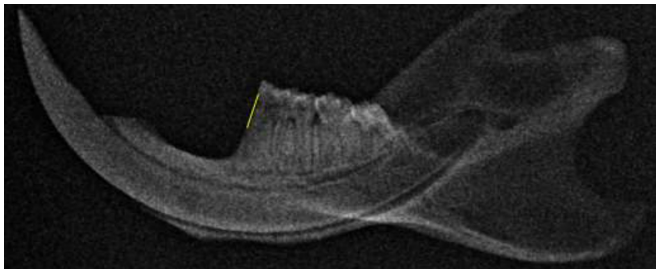


Figure 1. Radiograph of the hemimandible of 120-day-old Wister rats.

The yellow line shows the distance from the cementoenamel juntion to the alveolar bone crest on the mesial side of the left mandibular first molar, which was used for the demonstration of periodontitis.

Collection of EDL muscle

For collection of the EDL muscle, the skin of the pelvic limbs was separated and the tibialis anterior muscle was removed for dissection of the EDL muscle. The length (mm) of the muscle was measured with a digital caliper (Digimess®, São Paulo, Brazil) and the muscle was weighed on a digital scale. The EDL muscle was then cut into fragments and the right antimere was fixed in Methacarn for 24 hours and stored in 70% alcohol until the time of processing for histological analysis of muscle fibers and connective tissue. The left antimere was fixed in Karnovsky fixative (23) for the histochemical study of neuromuscular junctions (NMJs).

Histological study of muscle fibers and connective tissue

The EDL muscle was embedded in histological paraffin using the N-butyl alcohol protocol. The specimens were then cut transversely into 7-µm-thick semi-serial sections using a Leipzig microtome. The sections obtained were processed as described below.

For the study of muscle fibers, the sections were stained with hematoxylin-eosin (24). These slides were used for the quantification of nuclei and measurement of fiber area, major and minor muscle fiber diameters, nucleus/fiber ratio, and capillary/fiber ratio based on the analysis of 15 microscopic fields (40x objective) per animal. Only intact fibers in the microscopic fields were considered for the measurement of fiber area and nucleus quantification. For determination of the capillary/fiber ratio, muscle fibers covering the upper right margins were included in the count, while muscle fibers present in the lower left margins were excluded from the analysis. Two trained evaluators individually performed the quantification using the mean of the values obtained (25).

For the study of connective tissue, the sections were stained with Masson's trichrome (26), and the percentage of connective tissue was determined in 10 microscopic fields per animal (40x objective).

Morphological and morphometric study of neuromuscular junctions

For the study of NMJs, fragments of the left antimere of the EDL muscle fixed in Karnovsky solution were cut into three or four longitudinal sections with stainless-steel blades. The sections obtained were submitted to the nonspecific esterase reaction (27). For morphometric analysis of NMJs, the area and major and minor diameters of 100 NMJs per animal were measured on the microscopic images (20x objective).

Analysis of cholinesterase activity

The EDL muscle was frozen in liquid nitrogen and stored in a freezer at -80 °C. The samples were homogenized in 1 mL Tris-HCl buffer, pH 7.4, and centrifuged at 12,000 rpm for 10 minutes at 4 °C. Protein was quantified in the samples by the method of Bradford *et al.* (28) using bovine serum albumin as standard. All samples were then normalized to 1 mg protein/mL.

The neurotoxic effect of diseases was assessed by measuring the activity of cholinesterase (ChE) using the method of Ellman (29), adapted for microplates by Herbert (30). Acetylcholine was used as substrate and 5,5'-diethyl-bis-(2-nitrobenzoic acid) (DTNB) as color reagent. Absorbance was read in a spectrophotometer at a wavelength of 405 nm, with four readings over 3 minutes. Enzyme activity was expressed as nmol hydrolyzed acetylthiocholine min^{-1} mg $protein^{-1}$.

Image analysis

For the morphometric study of muscle fibers, connective tissue and NMJs, the images were captured with an Olympus DP71 camera (Tokyo, Japan) coupled to an Olympus Bx60® microscope using the DP Controler 3.2.1 276 program. Morphometric analysis was performed using the Image Pro Plus 6.0® program (Media Cybernetics, Maryland, USA).

Statistical analysis

The results were analyzed statistically using the XLSTAT 2014.5.03 software by Addinsolt. The normality distribution of all variables was tested. Data showing a normal distribution were compared by two-way ANOVA, followed by Tukey's multiple comparisons post-test. The Kruskal-Wallis test, followed by Dunn's post-test, was used for non-normally distributed data. The results were expressed as the mean ± standard deviation. A P-value < 0.05 was considered to be significant.

RESULTS

Study of dams

Body parameters

Animals of the MSG group exhibited a reduction of 18% ($p < 0.0001$) in body weight and of 11% ($p < 0.0001$) in nasoanal length compared to the CTL group. There was an increase of 106% ($p < 0.0001$) in retroperitoneal and periepididymal fat weights in the MSG group compared to the CTL group. Comparison of the MSG-PD and PD

Table I. Body parameters of 77-day-old dams of the control (CTL), MSG-induced obesity (MSG), periodontitis (PD), and MSG-induced obesity + periodontitis (MSG/PD) groups.

Body parameters	CTL (n = 10)	MSG (n = 7)	PD (n = 14)	MSG/PD (n = 7)
Body weight (g)	245.0 ± 13.8[a]	200.9 ± 21.3[b]	257.5 ± 17.8[a]	200.9 ± 20.1[b]
Nasoanal length (cm)	19.4 ± 0.52[a]	17.3 ± 0.39[b]	19.0 ± 0.88[a]	17.5 ± 0.58[b]
Lee index	322.6 ± 7.68[a]	338.6 ± 15.21[a]	337.7 ± 19.36[a]	334.6 ± 12.51[a]
Retroperitoneal and periepididymal fat (%)	1.71 ± 0.53[a]	3.53 ± 1.03[b]	1.84 ± 0.61[a]	2.82 ± 0.33[b]

Values are experssed as mean ± standard deviation. The Kruskal-Wallis test and Dunn's post-test were used for the comparison of nasoanal length and two-way ANOVA followed by Tukey's post-test for the other variables. Different letters indicate a significant difference ($p < 0.05$).

Table II. Macroscopic parameters of 120-day-old offspring of the control (CTL-F1), MSG-induced obesity (MSG-F1), periodontitis (PD-F1), and MSG-induced obesity + periodontitis (MSG/PD-F1) groups.

Macroscopic parameters	CTL-F1 (n = 7)	MSG-F1 (n = 7)	PD-F1 (n = 7)	MSG/PD-F1 (n = 8)
Body weight (g)	384.9 ± 33.6[a]	352.9 ± 20.2[a]	390.9 ± 37.9[b]	354.5 ± 14.3[a]
Nasoanal length (cm)	23.6 ± 0.69[a]	23.4 ± 0.63[a]	23.8 ± 0.86[a]	23.4 ± 0.52[a]
Lee index	307.5 ± 8.74[a]	302.5 ± 7.98[a]	307.2 ± 5.94[a]	302.8 ± 5.24[a]
Retroperitoneal and periepididymal fat (%)	2.96 ± 0.24 [ab]	2.61 ± 0.31[a]	3.11 ± 0.35[b]	2.13 ± 0.51[c]
EDL muscle weight (mg)	163.7 ± 15.8[a]	149.1 ± 11.0[a]	164.7 ± 18.6[a]	147.8 ± 16.0[a]
EDL muscle length (mm)	28.8 ± 1.43[a]	26.8 ± 1.41[a]	26.2 ± 1.22[a]	20.5 ± 8.24[b]

Values are expressed as mean ± standard deviation. Two-way ANOVA and Tukey's post-test. Different letters indicate a significant difference ($p < 0.05$).

groups showed a reduction of 22% ($p < 0.0001$) in body weight and of 8% ($p < 0.0001$) in nasoanal length in the former. The MSG-PD group exhibited a 53% increase ($p < 0.0001$) in retroperitoneal and periepididymal fat weights when compared to the PD group (**table I**).

Radiographic analysis

Radiographic analysis of the hemimandibles revealed greater alveolar bone loss in the groups submitted to PD induction (PD and MSG/PD groups) compared to the CTL and MSG groups; however, obesity did not exacerbate bone loss in the MSG-PD group. Bone loss was 61% higher ($p < 0.0001$) in the PD group compared to the CTL group, but 24% ($p < 0.0317$) lower in the MSG/PD group compared to the PD group (**figure 2**).

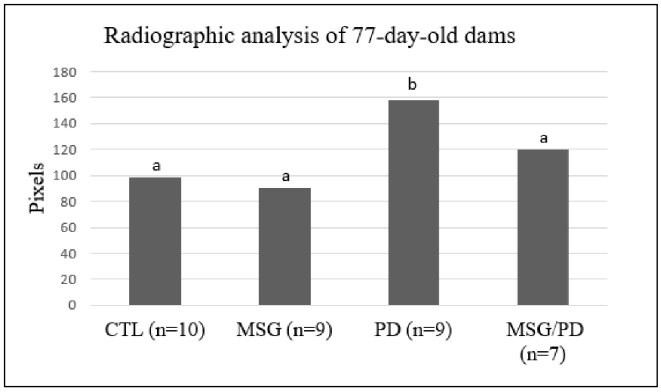


Figure 2. Radiographic analysis of 77-day-old dams of the control (CTL), MSG-induced obesity (MSG), periodontitis (PD), and MSG-induced obesity + periodontitis (MSG/PD) groups.

Table III. Microscopic parameters of the extensor digitorum longus muscle of 120-day-old offspring of the control (CTL-F1), MSG-induced obesity (MSG-F1), periodontitis (PD-F1), and MSG-induced obesity + periodontitis (MSG/PD-F1) groups.

Microscopic parameters	CTL-F1 (n = 6)	MSG-F1 (n = 6)	PD-F1 (n = 6)	MSG/PD-F1 (n = 6)
Muscle fiber area (µm2)	2114.1 ± 420.9[a]	2343.5 ± 293.2[a]	2320.4 ± 295.5[a]	2373.9 ± 167.6[a]
Major diameter of the muscle fiber (µm)	63.4 ± 7.49[a]	68.1 ± 5.42[a]	68.3 ± 7.45[a]	67.0 ± 4.25[a]
Minor diameter of the muscle fiber (µm)	40.4 ± 4.05[a]	42.6 ± 2.32[a]	42.0 ± 1.84[a]	42.8 ± 0.76[a]
Fiber density	541 ± 102.9[a]	469 ± 47.0[a]	451 ± 29.2[b]	464 ± 29.2[a]
Number of peripheral nuclei	710 ± 116.5[a]	664 ± 47.2[a]	669 ± 64.2[a]	699 ± 67.4[a]
Number of central nuclei	1.17 ± 1.2[a]	2.7 ± 1.3[a]	3.0 ± 1.8[a]	2.5 ± 1.4[a]
Nucleus/fiber ratio	1.32 ± 0.07[a]	1.42 ± 0.06[a]	1.48 ± 0.19[a]	1.50 ± 0.13[a]
Total number of capillaries	67.3 ± 7.53[a]	74.2 ± 9.23[a]	82.2 ± 23.57[a]	71.8 ± 26.44[a]
Capillary/fiber ratio	0.13 ± 0.03[a]	0.16 ± 0.01[a]	0.18 ± 0.04[b]	0.14 ± 0.04[a]
Connective Tissue (%)	2.95% ± 0.33[a]	4.46% ± 0.26[b]	3.48% ± 0.34[a]	4.36% ± 0.39[b]

Values are expressed as mean ± standard deviation. Two-way ANOVA followed by Tukey's post-test. Different letters indicate a significant difference ($p < 0.05$).

Study of offspring

Macroscopic parameters

Animals of the MSG/PD-F1 group exhibited a 9% reduction ($p < 0.0248$) in body weight compared to the PD-F1 group. Retroperitoneal and periepididymal fat weights were reduced by 18% ($p < 0.0001$) in the MSG/PD-F1 group compared to the MSG-F1 group and by 31% ($p < 0.0001$) compared to the PD-F1. Regarding EDL muscle length, there was a reduction of 23% ($p < 0.0089$) in the MSG/PD-F1 group compared to the MSG-F1 group and of 21% ($p < 0.0089$) compared to the PD-F1 group. However, no significant differences in naso-anal length, Lee index or EDL muscle weight were observed between the groups studied (**table II**).

Radiographic analysis

Bone loss was 49% higher ($p < 0.0004$) in the PD-F1 group compared to the CTL group confirming the onset of the disease. A 35% higher bone loss was observed in the MSG/PD-F1 group compared to the MSG-F1 group. There was no significant difference between the other groups (**figure 3**).

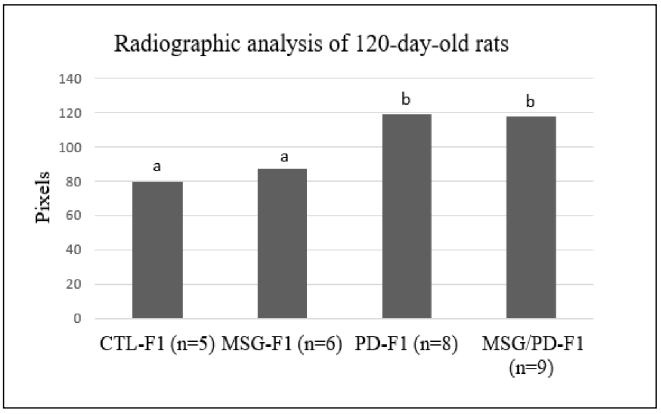


Figure 3. Radiographic analysis of 120-day-old rats of the control (CTL-F1), MSG-induced obesity (MSG-F1), periodontitis (PD-F1), and MSG-induced obesity + periodontitis (MSG/PD-F1) groups.

Morphological and morphometric analysis of muscle fibers

Morphological analysis of the EDL muscle showed preserved fiber morphology in the CTL group, including maintenance of the polygonal shape, fascicular arrangement and multinucleated cells with peripheral nuclei (**figure 4A**).

Some muscle fibers with central nuclei were observed in the MSG-F1, PD-F1, and MSG/PD-F1 groups (**figure 4B,E,G**). The fibers had an amorphous shape and the sarcoplasm was differentially stained, which was more expressive in the MSG/PD-F1 group (**figure 4C,D,F,H,I**).

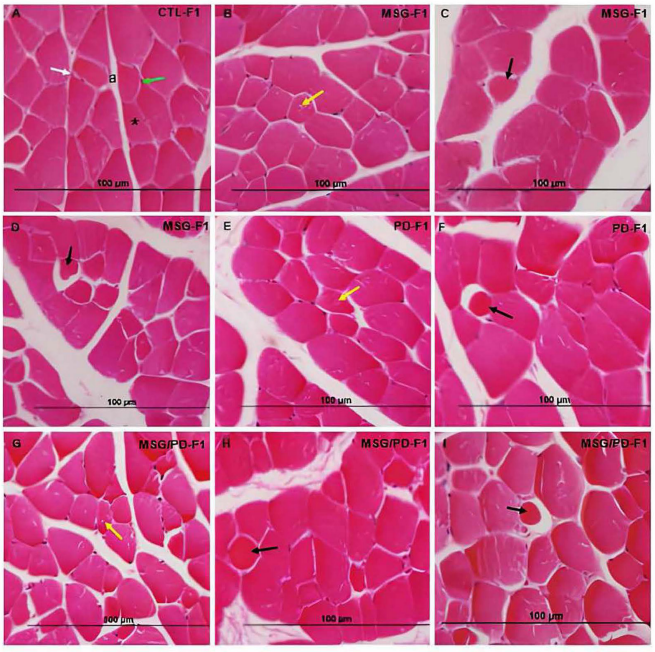


Figure 4. Photomicrographs of cross-sections of the extensor digitorum longus muscle of rats at 120 days of age.
Hematoxylin-eosin. Control group (CTL-F1), MSG-induced obesity group (MSG-F1), periodontitis group (PD-F1), and MSG-induced obesity + periodontitis group (MSG/PD-F1). (**A**) Muscle fibers with a polygonal shape (asterisk), peripheral nucleus (green arrow), perimysium (letter a), and capillary (white arrow). (**B, E, G**) Central nucleus (yellow arrow). (**C, D, F, H, I**) Amorphous fiber (black arrow).

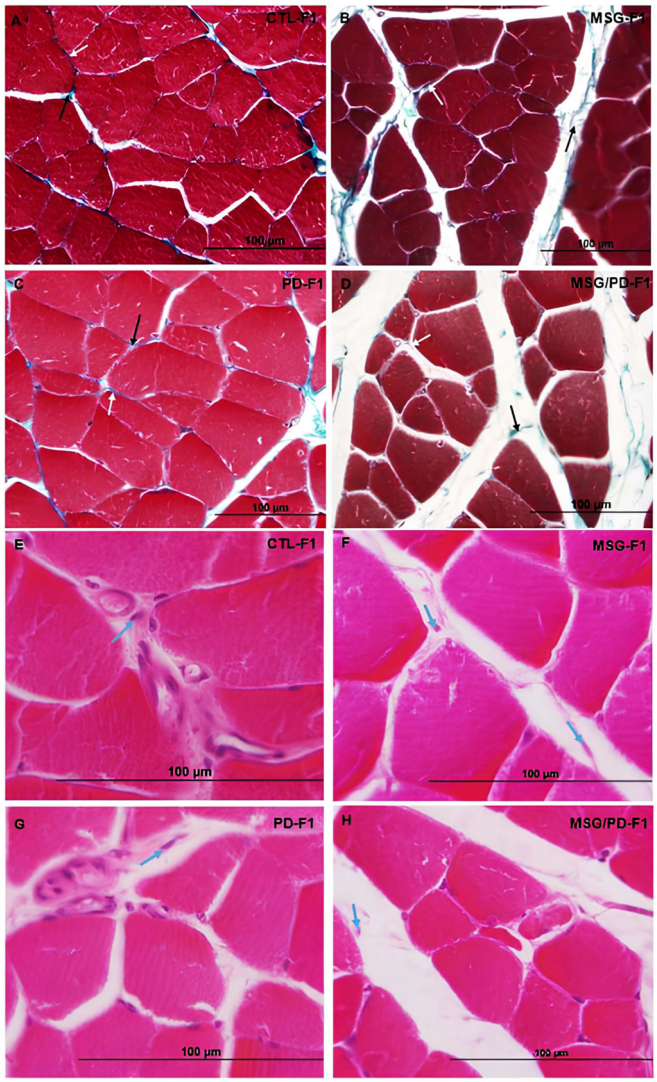


Figure 5. Photomicrographs of cross-sections of the extensor digitorum longus muscle of rats at 120 days of age.
Control group (CTL-F1), MSG-induced obesity group (MSG-F1), periodontitis group (PD-F1), and MSG-induced obesity + periodontitis group (MSG/PD-F1). (**A-D**) Observe connective tissue in the perimysium (black arrow) and endomysium (white arrow). Masson's trichrome. (**E-H**) Observe fibroblasts in connective tissue. Hematoxylin-eosin.

Fibroblasts were observed in the connective tissue of all groups studied (CTL-F1, MSG-F1, PD-F1, and MSG/PD-F)1 (**figure 5E,F,G,H**).
Morphometric analysis of EDL muscle fibers showed a 17% reduction ($p < 0.0775$) in fiber density in the PD-F1 group compared to the CTL-F1 group. The capillary/fiber ratio was increased by 38% ($p < 0.0697$) in the PD-F1 group compared to the CTL-F1 group. However, there were no significant differences between the four groups studied in terms of muscle fiber area, major and minor diameter, peripheral and central nuclei, nucleus/fiber ratio, total number of capillaries, or capillary/fiber ratio (**table III**).

Analysis of connective tissue

Connective tissue was detected in the perimysium and endomysium of the four groups (**figure 5A,B,C,D**), with a predominance in the perimysium of the MSG-F1 and MSG/PD-F1 groups (**figure 5B,D**). The results of connective tissue estimation showed a significant increase of 51% ($p < 0.0001$) in the MSG-F1 group when compared to the CTL-F1 group. Animals of the MSG/PD-F1 group exhibited an increase of 25% ($p < 0.0301$) compared to the PD-F1 group. There was no significant difference between the PD-F1 and CTL-F1 groups or between the MSG/PD-F1 and MSG-F1 groups (**table III**).

Table IV. Morphometric parameters of the neuromuscular junctions (NMJs) of the extensor digitorum longus (EDL) muscle of 120-day-old offspring of the control (CTL-F1), MSG-induced obesity (MSG-F1), periodontitis (PD-F1), and MSG-induced obesity + periodontitis (MSG/PD-F1) groups.

Morphometric parameters	CTL-F1 (n = 7)	MSG-F1 (n = 7)	PD-F1 (n = 7)	MSG/ PD-F1(n = 7)
Area of NMJs (µm2)	462.1 ± 124.0a	383.9 ± 84.9a	372.0 ± 69.8a	392.5 ± 109.1a
Major diameter of the NMJs (µm)	39.5 ± 4.7a	35.4 ± 4.1a	37.2 ± 3.4a	37.2 ± 4.3a
Minor diameter of the NMJs (µm)	18.1 ± 3.3a	15.5 ± 2.5a	16.4 ± 2.1a	17.4 ± 2.9 a
ChE enzyme activity (Nmol.min-1.mg of protein-1)	5.7 ± 0.8a	5.7 ± 1.7a	5.6 ± 1.2a	5.6 ± 1.1a

Values are expressed as mean ± standard deviation. Two-way ANOVA followed by Tukey's post-test. Different letters indicate a significant difference ($p < 0.05$).

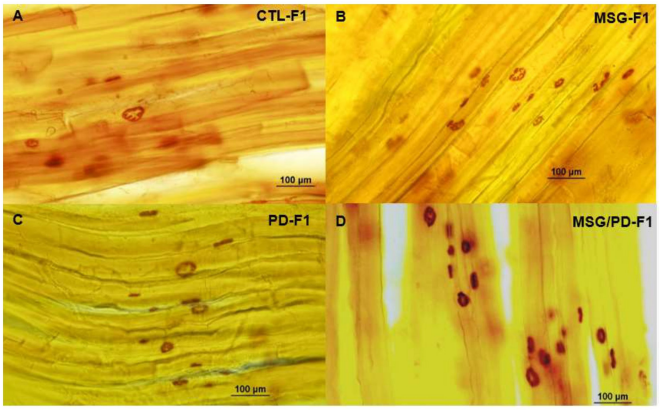


Figure 6. Photomicrographs of neuromuscular junctions (NMJs) in longitudinal sections of the extensor digitorum longus muscle of rats at 120 days of age.

Nonspecific esterase. Control group (CTL-F1), MSG-induced obesity group (MSG-F1), periodontitis group (PD-F1), and MSG-induced obesity + periodontitis group (MSG/PD-F1). (**A-D**) Observe the NMJs with oval, elliptical, and round shapes.

Morphologic and morphometric analysis of NMJs in EDL muscle

The animals of all groups studied exhibited NMJs with elliptical, oval, and round shapes (**figure 6A-D**) and no changes in morphology were observed. Morphometric analysis revealed no significant differences in the area or major or minor diameter of the NMJs between the groups studied (**table IV**).

Analysis of cholinesterase activity

There were no significant differences in ChE enzymatic activity between the groups studied ($p>0.05$) (**table IV**).

DISCUSSION

The present study demonstrated a reduction of 18% in body weight and of 11% in nasoanal length in dams submitted to obesity induction (MSG group) compared to the CTL group. In contrast, the group of dams submitted to the induction of obesity and PD (MSG/PD group) exhibited a reduction of 22% in body weight and of 8% in nasoanal length compared to the PD group. These findings can be explained by the neurotoxic effect of MSG, which causes lesions in the hypothalamus that can reduce the production of growth hormone-releasing hormone, with a consequent decrease in the circulating levels of growth hormone. The latter is responsible for the growth of body tissues and its reduced secretion can result in stunted growth and shorter body length and lower body weight and muscle mass (19, 31). The results of this study agree with the literature. For example, Mattia *et al.* (32), who evaluated the effect of MSG and ligature-induced PD on periodontal tissues of Wistar rats, observed body weight loss in animals of the obese and obese with PD groups.

An increase in retroperitoneal and periepididymal fat weights was observed in the MSG group compared to the CTL group and in the MSG/PD group compared to the PD group, confirming obesity. These results corroborate the findings of Coradini *et al.* (33) who observed an increase in both types of fats in Wistar rats with MSG-induced obesity. This finding can be explained by the fact that the hypothalamus is the organ that regulates food intake and energy expenditure. Lesions in this region caused by excess MSG can cause dysfunction of the hypothalamic-pituitary axis and one consequence of this dysfunction is excessive fat accumulation (34).

Radiographic analysis of maternal alveolar bone loss revealed greater bone resorption in the groups submitted

to PD induction compared to the other groups, confirming the onset of the disease. However, bone loss was 24% lower in the MSG-PD group when compared to the PD group, suggesting that MSG-induced obesity exerts a protective effect on alveolar bone loss. The present results corroborate the findings of other studies (10, 32, 35). The protective effect of obesity on bone tissue can be explained by the higher concentration of insulin in obese individuals since osteoblasts possess an insulin receptor that stimulates osteogenic differentiation and inhibits osteoclastogenesis (36).

Numerous studies have sought to understand the effect of maternal alterations such as obesity and PD on the offspring (37, 38). However, few studies have investigated the association between the two variables and their effects on skeletal muscle. In the present study, analysis of macroscopic parameters of the offspring revealed no significant difference in nasoanal length, Lee index, or EDL muscle weight between the groups studied. However, the MSG/PD-F1 group exhibited a 9% reduction in body weight when compared to the PD-F1 group. Retroperitoneal and periepididymal fat weights were reduced by 18% in the MSG/PD-F1 group compared to the MSG-F1 group and by 31% compared to the PD-F1 group. Animals of the MSG/PD-F1 group also exhibited a reduction of 23% in EDL muscle length compared to the MSG-F1 group and of 21% compared to the PD-F1 group. The results suggest that obesity did not develop in the offspring over the period of the experiment. Studies using the same experimental model of maternal obesity have shown that the offspring start to develop obesity by 5 months of life (approximately 150 days) (39, 40), while the offspring in this study were euthanized at 120 days of life (approximately 4 months). However, the alteration in muscle length suggests that the association of systemic inflammatory diseases can lead to muscle changes.

Fetal programming suggests that the occurrence of insults during perinatal life (first "hit") would not be sufficient to modify the adult phenotype. However, exposure to stressors during postnatal life would act as a second "hit" and could unmask or potentiate the effects of fetal programming (41). In the present study, the offspring of dams with induced PD were also submitted to induction of the diseases. Bone loss was 49% higher in animals of the PD-F1 group when compared to the CTL-F1 group, demonstrating the onset of the disease. The 35% higher bone loss in animals of the MSG/PD-F1 group compared to the MSG-F1 group also confirmed the onset of the disease; however, obesity did not exacerbate this bone loss.

Muscle tissue is characterized by high plasticity and some stimuli can trigger morphological, functional, and metabolic changes. Thus, phenotypic adaptation of the muscle can occur in different situations, such as nutritional alterations, resistance exercise, electrical stimulation, aging, and heat stress (42). In the present study, morphological analysis of the muscle fibers revealed point alterations such as amorphous fibers with differentially stained sarcoplasm in the groups submitted to the induction of obesity and PD (MSG-F1, PD-F1, and MSG/PD-F1), which was more expressive in the groups with both diseases. These changes suggest a process of muscle degeneration that starts with the loss of cell shape as a result of the reorganization of sarcomeres that occurs during the adaptation process (43). Few studies have analyzed the skeletal muscle of offspring born to rats with obesity and PD. Boaretto *et al.* (44) evaluated the effects of MSG-induced obesity on the soleus muscle of adult Wistar rats and observed the presence of amorphous fibers in obese animals; however, the authors did not find differentially stained sarcoplasm. We therefore suggest that the skeletal muscle alterations found in the present study may be due to fetal programming.

Animals of the MSG-F1, PD-F1 and MSG/PD-F1 groups exhibited central nuclei indicative of muscle fiber regeneration, which is the result of enhanced cell activity to increase the protein synthesis rate. The presence of nuclear activity in this tissue may indicate adaptive mechanisms after cell damage (45). Leite *et al.* (46), who evaluated the effect of ligature-induced PD on the soleus muscle of adult Wistar rats, also reported this alteration. These muscle fiber changes may be the results of fetal programming.

The results of morphometric analysis of the muscle fibers showed a 17% reduction in fiber density and a 38% increase in the capillary/fiber ratio in the PD-F1 group when compared to the CTL-F1 group. The first phase of the tissue repair process is characterized by an increase in vascularization, which is necessary to increase the blood supply to the skeletal muscle tissue (47). Hence, the results suggest that the increase in the capillary/fiber ratio in animals with PD was an attempt to trigger tissue repair.

Connective tissue is synthesized by fibroblasts and is located between muscle fibers. It is the main component of the extracellular matrix and plays a key role in maintaining the integrity of muscle fibers. However, excess connective tissue can influence muscle function (48). In the present study, there was an increase in the percentage of connective tissue in animals that received MSG administration, with an increase of 51% in the MSG-F1 group compared to the CTL-F1 group and of 25% in the MSG/PD-F1 group compared to the PD-F1 group. Similar results have been reported by Boaretto *et al.* (44) who evaluated the effect of

MSG-induced obesity on the soleus muscle of adult Wistar rats and observed an increase in connective tissue in obese animals. The increase in connective tissue may be related to the reduction in muscle fiber density as seen in the present study. Furthermore, excess connective tissue may have been a result of fetal programming due to obesity.

There were no morphological or morphometric alterations in NMJs between the groups studied. Animals submitted to the induction of obesity and PD, alone or in combination, exhibited a smaller area and smaller major and minor diameters compared to the CTL-F1 group, although the differences were not statistically significant. Studies report alterations in the size of NMJs in metabolic and genetic diseases (49). However, few studies have analyzed NMJs in the offspring of rats with obesity and PD. Studying the diaphragm muscle of Wistar rats with MSG-induced obesity, Oliveira *et al.* (50) found a reduction in the area and major diameter of the NMJs.

Obesity and PD are associated with low-grade systemic inflammation (10, 12), which causes an increase in inflammatory markers such as interleukin 6. Excess levels of this marker lead to a reduction in insulin-like growth factor 1 signaling (51), which plays an important role in the development and differentiation of myoblasts and in the neuromuscular system (52). The reduction in the NMJ parameters observed in the offspring of this study may have been due to the alterations caused by inflammation present in the dams, which triggered fetal programming and affected NMJ development.

Regarding the activity of ChE, there were no significant differences between the groups studied, suggesting that obesity and PD did not alter the amount of ChE in the synaptic cleft, did not induce changes in neurotransmission, and did not cause toxicity that would be characterized by the inhibition of enzymatic activity (52). Therefore, neither obesity nor PD interfered with offspring development in this study, maintaining neuromuscular integrity.

CONCLUSIONS

In view of the present results, we conclude that fetal programming due to obesity and PD exerted effects on EDL muscle fibers and connective tissue. In addition, the association of obesity and PD affected body parameters and EDL muscle length in the offspring, suggesting that inflammatory diseases can cause body and muscle changes. Obesity and PD, alone or in combination, also promoted degenerative changes in muscle fibers, which could compromise muscle function. Obesity led to an increase in the percentage of connective tissue, which was more expressive in the group submitted only to obesity induction, influencing the mechanism of tissue regeneration. There were no alterations in ChE activity. Furthermore, no significant differences in NMJ parameters were observed; however, the results showed a reduction in the total area and major and minor diameters in the groups with obesity and PD alone or in combination, suggesting alterations in muscle function.

FUNDINGS

This work was carried out with financial support from the Coordination for the Improvement of Higher Education Personnel - Brazil (CAPES).

DATA AVAILABILITY

Data are available under reasonable request to the corresponding author.

CONTRIBUTIONS

GLC, MMT: writing – original draft. TNPP, MGK, RCLS, CAN, SLB: methodology. RMCB, LFCR: results. ATBG: formal analysis.

CONFLICT OF INTERESTS

The authors declare that they have no conflict of interests.

REFERENCES

1. Barker DJ. P. The origins of the developmental origins theory. J Intern Med. 2007;261(5):412-7. doi 10.1111/j.1365-2796.2007.01809.x.
2. Silveira PP, Portella AK, Goldani MZ, Barbieri MA. Developmental origins of health and disease (DOHaD). J Pediatr. 2007;83(6):494-504. doi 10.2223/JPED.1728.
3. Marciniak A, Patro-Malysza A, Kimber-Trojnar Z, Marciniak B, Oleszczuk J, Leszczynska-Gorzelak B. Fetal programming of the metabolic syndrome. Taiwan J Obstet Gynecol. 2017;56(2):133-8. doi: 10.1016/j.tjog.2017.01.001.
4. Carolan-Olah M, Duarte-Gardea M, Lechuga J. A critical review: early life nutrition and prenatal programming for adult disease. J Clin Nurs. 2015;24(23-24):3716-29. doi: 10.1111/jocn.12951.
5. Urrutia-Pereira M, Solé D. Deficiência de vitamina D na gravidez e o seu impacto sobre o feto, o recém-nascido e na infância. Rev Paul Pediatr. 2015;33(1). doi: 10.1016/j.rpped.2014.05.004.

6. Who. World Health Organization. 2018. Obesity. Available at: https://www.who.int/topics/obesity/en/. Last access date: 03/07/2024.
7. Brasil, Ministério da Saúde. Pesquisa nacional de saúde: 2019 – Atenção primária à saúde e informações antropométricas: Brasil / IBGE, Coordenação de Trabalho e Rendimento. Rio de Janeiro: IBGE, 2020.
8. Dimitrov IV, Stankova TR, Angelova PA, et al. Inflammatory Response of Skeletal Muscles to a High-Fat Diet. Muscles Ligaments Tendons J. 2022;12(4):490-6. doi 10.32098/mltj.04.2022.04.
9. White PAS, Brito LC. Model of high-fat diet-induced obesity associated to insulin resistance and glucose intolerance. Arq Bras Endocrinol Metabol. 2013;57(5):339-45. Portuguese. doi: 10.1590/s0004-27302013000500002.
10. Brandelero S, Bonfleur ML, Ribeiro RA, et al. Decreased TNF-α gene expression in periodontal ligature in MSG-obese rats: A possible protective effect of hypothalamic obesity. Arch Oral Biol. 2012;57(3):300-6. doi: 10.1016/j.archoralbio.2011.08.024.
11. Global burden of disease study. Incidência global, regional e nacional, prevalência e anos vividos com incapacidade para 328 doenças e lesões para 195 países, 1990-2016: uma análise sistemática para o Estudo Global de Carga de Doenças. Lanceta. 2016. doi: 10.1016/S0140-6736(17)32154-2.
12. Genco R, Grossi SG, Ho A, Nishimura F, Murayama Y. A Proposed Model Linking Inflammation to Obesity, Diabetes, and Periodontal Infections. J Periodontol. 2005;76(11):2075-84. doi: 10.1902/jop.2005.76.11-S.2075.
13. Dahiya P, Kamal R, Gupta R. Obesity, periodontal and general health: Relationship and management. Indian J Endocrinol Metab. 2012;16(1):88-93. doi 10.4103/2230-8210.91200.
14. De Castilhos ED, Horta BL, Gigante DP, Demarco FF, Peres KG, Peres MA. Association between obesity and periodontal disease in young adults: a population-based birth cohort. J Clin Periodontol, 2012;39(8):717-24. doi 10.1111/j.1600-051X.2012.01906.x.
15. Moura-Grec PG, Marsicano JA, Carvalho CAP, Sales-Peres SHC. Obesity and perídontitis: systematic review and meta-analysis. Cien Saude Colet. 2014;19(6):1763-72. doi: 10.1590/1413-81232014196.13482013.
16. Lagas IF, Nijst BKJF, Hartgens F, et al. Lower Extremity Tendinopathies are Associated with Metabolic and Chronic Diseases: A Systematic Review. Muscles Ligaments Tendons J. 2024;14(1):102-30. doi 10.32098/mltj.01.2024.10.
17. Frontera WR, Ochala J. Skeletal muscle: a brief review of structure and function. Calcif Tissue Int. 2015;96(3):183-95. doi: 10.1007/s00223-014-9915-y.
18. Ward SS, Stickland NC. Why are slow and fast muscles differentially affected during prenatal undernutrition? Muscle Nerve. 1991;14(3):259-67. doi: 10.1002/mus.880140310.
19. Olney J. Brain lesions, obesity, and other disturbances in mice treated with monosodium glutamate. Science. 1969;164(3880):719-21. doi: 10.1126/science.164.3880.719.
20. Nassar PO, Nassar CA, Guimarães MR, et al. Simvastatin therapy in cyclosporine A-induced alveolar bone loss in rats. J Periodontal Res. 2009;44(4):479-88. doi: 10.1111/j.1600-0765.2008.01143.x.
21. Lee HJ, Jun JK, Lee SM, Ha JE, Paik D, Bae KH. Association Between Obesity and Periodontitis in Pregnant Females. J Periodontol. 2014;85(7):224-31. doi: 10.1902/jop.2014.130578.
22. Bernardis LL, Patterson BD. Correlation between'Lee index'and carcass fat content in weanling and adult female rats with hypothalamic lesions. J Endocrinol. 1968;40(4):527-8. doi: 10.1677/joe.0.0400527.
23. Karnovski MJ. A formaldehyde-glutaraldehyde fixative of high osmolality for use in electron microscopy. J Cell Biol. 1965;27:1-149.
24. Junqueira LC, Junqueira LMM. Técnicas básicas de citologia e histologia. São Paulo: Universidade de São Paulo, 1983.
25. Fernandes T, Roque FR, Magalhães FC, Carmo EC, Oliveira EM. O treinamento físico aeróbico corrige a rarefação capilar e as alterações nas proporções dos tipos de fibra muscular esquelética em ratos espontaneamente hipertensos. Revista Brasileira de Medicina do Esporte. 2012;18(4):267-72. doi: 10.1590/S1517-86922012000400010.
26. Bancroft JD, Steven A. Theory and practice of histological techniques. 3rd ed. Churchill Livingstone: Edinburg. 1990.
27. Lehrer GM, Ornstein L. A diazo coupling method for the eléctron microscopic localization of cholinesterase. J Biophys Biochem Cytol. 1959;6:399-419. doi: 10.1083/jcb.6.3.399.
28. Bradford MM. A rapid and sensitive method for the quantitation of microgram quantities of protein utilizing the principle of protein-dye binding. Anal Biochem. 1976;16:248-54. doi: 10.1016/0003-2697(76)90527-3.
29. Ellman GL, Courtney KD, Jr VA, Feather-Stone RM. A new and rapid colorimetric determination of acetylcholinesterase activity. Biochem. Pharmacol. 1961;7:88-95. doi: 10.1016/0006-2952(61)90145-9.
30. Herbert A. Acetylcholinesterase activity in aquatic organisms as pollution biomarker. Angew Zool. 1995;3:1-5. doi:10.5894/rgci430.
31. Maiter D, Underwood LE, Martin JB, Koenig JI. Neonatal Treatment with Monosodium Glutamate: Effects of Prolonged Growth Hormone (GH)-Releasing Hormone Deficiency on Pulsatile GH Secretion and Growth in Female Rats. Endocrinology. 1991;128:1100-6. doi: 10.1210/endo-128-2-1100.
32. Mattia TM, Leite MA, Nassar PO, et al. The Influence of Obesity Induced by Monosodium Glutamate in Periodontal Tissues of Female Wister Rats with Experimental Periodontitis. Am Int J Contemp Res. 2017;7(3):28-40.
33. Coradini JG, Karvat J, Brancalhão RMC, Ribeiro LFC, Bonfleur ML, Bertolini GRF. Características nociceptivas e histomorfométricas de nervos medianos de ratos com obesidade induzida pelo glutamato monossódico. Scientia Medica. 2014;24(4):368-72. doi: 10.15448/1980-6108.2014.4.18429.
34. Bonfleur ML, Ribeiro RA, Pavallo A, et al. Duodenal-jejunal by-pass restores insulin action and betacell function in hypothalamic-obese rats. Obes Surg. 2015;25:656-65. doi: 10.1007/s11695-014-1427-3.
35. Costa KF, Bonfleur ML, Pontillo V, et al. Evaluation of Periodontal Tissues and Abdominal Aorta of Rats with Induced Obesity by Monosodium Glutamate and Experimental Periodontitis. J Adv Med Med Res. 2017;19(2):1-14. doi: 10.9734/BJMMR/2017/30165.
36. Zhao LJ, Jiang H, Papasian CJ, et al. Correlation of obesity and osteoporosis: effect of fat mass on the determination

of osteoporosis. J Bone Miner Res. 2008;23(1):17-29. doi: 10.1359/jbmr.070813.
37. Manrique-Corredor EJ, Orozco-Beltran D, Lopez-Pineda A, Quesada JA, Gil-Guillen VF, Carratala-Munuera C. Maternal periodontitis and preterm birth: Systematic review and meta-analysis. Community Dent Oral Epidemiol. 2019;47(3):243-51. doi: 10.1111/cdoe.12450.
38. Vickers MH. Developmental Programming and Transgenerational Transmission of Obesity. Ann Nutr Metab. 2014;64(1):26-34. doi: 10.1159/000360506.
39. Campos KE, Sinzato YK, Pimenta W de P, Rudge MV, Damasceno DC. Effect of maternal obesity on diabetes development in adult rat offspring. Life Sci. 2007;81(19-20):1473-8. doi: 10.1016/j.lfs.2007.09.016.
40. Campos KE, Volpato GT, Calderon IM, Rudge MV, Damasceno DC. Effect of obesity on rat reproduction and on the development of their adult offspring. Braz J Med Biol Res. 2008;41(2):122-5. doi: 10.1590/s0100-879x2008005000001.
41. Puttabyatappa M, Cardoso RC, Padmanabhan V. Effect of maternal PCOS and PCOS-like phenotype on the offspring's health Mol Cell Endocrinol. 2016;5 (435): 29-39. doi: 10.1016/j.mce.2015.11.030.
42. Aguiar AF, Aguiar DH. Plasticidade muscular no exercício físico. R Bras Ci e Mov. 2009;17(3):104-13. doi: 10.18511/rbcm.v17i3.1226.
43. Coutinho EL, Gomes ARS, França CN, Oishi J, Salvini TF. Effect of passive stretching on the immobilized soleus muscle fiber morphology. J Med Biol Res. 2004;37(12):1853-61. doi: 10.1590/S0100-879X2004001200011.
44. Boaretto ML, Andrade BZ, Maciel JIHN, et al. Effects of vibratory platform training on the histomorphometric parameters of the soleus muscle in obese Wistar rats. Sport Sci Health. 2020;16:501-10. doi: 10.1007/s11332-020-00632-8.
45. Gundersen K. Muscle memory and a new cellular model for muscle atrophy and hypertrophy. J Exp Biol. 2016;219 (Pt 2):235242. doi: 10.1242/jeb.124495.
46. Leite MA, Mattia TM, Kakihata CMM, et al. Experimental periodontitis in the potentialization of the effects of immobilism in the skeletal striated muscle. Inflammation. 2017;40(6):2000-11. doi: 10.1007/s10753-017-0640-3.
47. Tidball JG. Regulation of muscle growth and regeneration by the immune system. Nat Rev Immunol. 2017;17(3):165-78. doi: 10.1038/nri.2016.150.
48. Slimani L, Micol D, Amat J, et al. The worsening of tibialis anterior muscle atrophy during recovery post-immobilization correlates with enhanced connective tissue area, proteolysis, and apoptosis. Am J Physiol Endocrinol Metab. 2012;303(11):E1335-47. doi: 10.1152/ajpendo.00379.2012.
49. Deschenes MR, Roby MA, Glass EK. Aging influences adaptations of the neuromuscular junction to endurance training. Neuroscience. 2011;190:56-66. doi: 10.1016/j.neuroscience.2011.05.070.
50. Oliveira MC. Efeito do treinamento com plataforma vibratória na morfologia do músculo diafragma em ratos com obesidade hipotalâmica [Dissertação on the Internet]. Cascavel: Universidade Estadual do Oeste do Paraná;2020. 111 s.
51. Caroni, P. Activity-sensitive signaling by muscle-derived insulin-like growth factors in the developing and regenerating neuromuscular system. Annals of the New York Academy of Sciences. 1993;692:209-22. doi: 10.1111/j.1749-6632.1993.tb26219.x.
52. Monteiro DA, Almeida JÁ, Rantin FT, Kalinin, AL. Oxidative stress biomarkers in the freshwater characid fish, Brycon cephalus, exposed to organophosphorus insecticide Folisuper 600 (methyl parathion). Comp Biochem Physiol C Toxicol Pharmacol. 2006;143(2):141-9. doi: 10.1016/j.cbpc.2006.01.004.